

# Carboxymethyl Starch: A Rheological Study

ROMANO LAPASIN,\* SABRINA PRICL, and PAOLO TRACANELLI

Department of Chemical, Environmental, and Raw Material Engineering, University of Trieste,  
Via Valerio 2, I-34127 Trieste, Italy

## SYNOPSIS

The rheological behavior of carboxymethyl starch aqueous systems has been studied under continuous and oscillatory shear conditions. The systems examined exhibited shear-dependent properties, typical of dispersions having a weak degree of particle aggregation. A transition in the rheological properties was observed with increasing concentration and/or decreasing temperature, as a consequence of formation of a three-dimensional continuous network in the disperse phase under rest conditions. The shear-dependent behavior changed from shear-thinning to plastic and a finite plateau appeared in the low frequency region of mechanical spectra. A rheological model was proposed for the correlation of both shear-thinning and plastic data, thus making possible an objective definition of the rheological transition. Oscillatory flow data confirmed the results obtained in continuous shear conditions, that is, the frequency dependence of the complex viscosity was almost parallel to the dependence of the steady shear viscosity on the rate of shear. Moreover, the high strain sensitivity of the viscoelastic quantities and their analysis in terms of relaxation spectra clearly indicated the moderate degree of connectivity of the structural network. © 1992 John Wiley & Sons, Inc.

## INTRODUCTION

As members of the biopolymers family, polysaccharides owe their broad commercial application to the extended range of functional properties, which are usually unique in their nature and often performed at low concentration levels.

The specific functional properties of polysaccharides are the result of their physical characteristics, which are primarily controlled by the molecular structure, that is, the monomeric units and the linkages joining them.

The ability of most polysaccharides to dissolve in water, thus changing the properties of their aqueous environment, coupled with their low toxicity, is responsible for most of their uses as hydrocolloids in the food, medical, and health care industries.

The carbohydrate polymers can also behave as thickeners, coating, drag-reducing and gel-forming agents. Moreover, polysaccharides perform, either by themselves or in association with other molecules (hormones, lipids or proteins) many vital biological functions by affording structural support and energy reserve, and by mediating various other processes such as adhesion, cellular recognition and growth.<sup>1</sup>

Among the many varieties of plant polysaccharides, one of the most abundant is starch. Starch is a complex substance that constitutes an energy fount essential in man and animal nutrition. The most important sources of starch are cereal grains, pulses, and tubers, where starch occurs as water insoluble granules. Starch is generally used to improve the functional properties of food products, but also finds applications in the formulation of glues, coatings, sizing and flocculating agents, chemicals, and building materials.

Chemically, starch itself consists of two classes of molecules, one linear, called amylose, the other branched, called amylopectin. Amylose is the minor

\* To whom correspondence should be addressed.

constituent by weight. Both molecules are based on repeated D-glucopyranose units, but amylose is mostly a linear  $\alpha$ -(1 $\rightarrow$ 4)-linked D-glucose, while amylopectin has both  $\alpha$ -(1 $\rightarrow$ 4) and  $\alpha$ -(1 $\rightarrow$ 6) linkages, which give origin to a highly branched polymer.

When an aqueous suspension of starch granules is heated above a certain temperature, known as the gelatinization temperature, irreversible swelling of the granules occurs, resulting predominantly in the release of amylose into solution. If the starch concentration is high enough, this polymer solution containing swollen granules behaves as a viscoelastic paste. On cooling, the paste thickens and becomes opaque and an elastic gel is formed. The pastes and gels may be regarded as composites consisting of a polymer solution or a gel filled with swollen granules.<sup>2</sup>

Carboxymethyl starch (CMS) is a synthetic derivative, obtained from starch by irreversible nucleophilic substitution using dialkylamino halides or epoxides, and is widely employed as additive in the paper industry and as thickener in the formulation of textile printing pastes.

Despite of the wide commercial use of starch, little work has been carried out to fully characterize aqueous systems containing starch carboxymethylated derivatives.<sup>3-7</sup>

The aim of the present article is to systematically investigate the flow behavior of carboxymethyl starch aqueous systems under steady and oscillatory flow conditions and to evaluate the effects of polymer concentration and temperature on the rheological properties of these systems.

## EXPERIMENTAL

### Materials

The pregelatinized carboxymethyl starch (CMS) used for this study was a commercial sample, sold under the trade name of Solvitose C 5F (AVEBE, The Netherlands), characterized by a degree of substitution (DS)  $0.34 \pm 0.01$  and a degree of polymerization (DP) of  $\sim 1250$  for amylose and  $\sim 1,500,000$  for amylopectin.

The effect of polymer concentration was studied on CMS at 25°C. The concentrations ( $C_p$ , %w/w) considered were the following: 2, 2.5, 2.8, 3.17, 4, and 6. All the systems were prepared by dissolving a proper amount of freeze-dried polymer in bidistilled water under gentle stirring. The concentration

was then determined by weighing both the lyophilized polymer and the final solution.

### Apparatus and Procedures

Experiments were performed on the systems prepared as reported in the previous section and left in the glass to rest overnight before use.

Continuous shear and dynamic measurements were carried out with two different rotational rheometers.

Under continuous shear conditions, data in the lower shear rate range ( $0.3\text{--}300\text{ s}^{-1}$ ) were obtained with a Haake Rotovisco RV100 measuring device CV100, equipped with a coaxial cylinder sensor system ZB15 (Couette type). During the tests, while the outer cup was driven, the inner cylinder was mechanically positioned and centered by an air bearing. Top and bottom surfaces were recessed to minimize end effects.

The Haake Rotovisco RV20 measuring device M5-Osc, equipped with a cone-and-plate system (PK5-0.5), was employed to expand the shear rate range up to  $6000\text{ s}^{-1}$ .

Stepwise procedures were applied for the analysis of the shear- and time-dependent properties in continuous shear flow conditions. The multiple step procedure consisted of a sequence of different shear rates,  $\dot{\gamma}$ . Each shear rate was kept constant until a steady value of the shear stress  $\tau$  was attained. The analysis of the shear-dependent behavior can be properly based upon the steady values of  $\tau$  obtained at different  $\dot{\gamma}$ , whereas the sequence of stress transients allows an evaluation of the extent of the time-dependent properties to be performed.

Stress-relaxation tests were carried out in order to determine the residual stress to be compared with the correspondent yield stress obtained from data fitting.

Oscillatory flow tests were carried out with the Haake Rotovisco RV20 (measuring device CV100, measuring system ZB15), in order to examine the viscoelastic properties of these systems.

During these tests, the outer cylinder was forced to oscillate sinusoidally at a frequency  $\omega$ , and the corresponding oscillation of the inner cylinder, proportional to the resultant torque, was recorded.

A dedicated software was used for data processing in order to correct the experimental data for inertial effects and to calculate the viscoelastic quantities, the complex modulus  $G^*$ , and the phase shift  $\delta$ .  $G^*$  can be resolved into its "in phase" (real part) and "90° out of phase" (imaginary part) components,

which yield the storage modulus  $G'$  and the loss modulus  $G''$ , respectively, according to the following relationships:

$$G' = G^* \cos \delta \quad (1)$$

$$G'' = G^* \sin \delta \quad (2)$$

Moreover,  $G^*$  can be converted into the complex viscosity  $\eta^*$  through:

$$\eta^* = \frac{G^*}{\omega} = \frac{\sqrt{(G')^2 + (G'')^2}}{\omega} \quad (3)$$

Frequency sweeps under simple oscillatory flow conditions were performed on each sample in a frequency range of 0.314 to 12.56 rad/s at two constant strain values  $\gamma^0$ , 0.24, and 2.4, respectively.

The strain dependence of the viscoelastic quantities was investigated through strain sweeps in the range 0.24–2.4 at two frequencies ( $\omega = 0.628$  and 6.28 rad/s).

Measurements were carried out in the temperature range 20–40°C in order to evaluate the temperature effect on the rheological properties of CMS systems.

## RESULTS AND DISCUSSION

### Continuous Shear Flow Tests

Transient tests in steady shear conditions were performed to evaluate if these materials exhibit time-dependent properties, that is, if they are characterized by any large scale structure. No evidence of

strong flow induced modifications of long range structures, with associated long formation or destruction time constants, was observed. The degree of structural deformation adjusted quickly, as indicated by the rapid approach of the shear stress  $\tau$  to a new steady value, when the shear rate  $\dot{\gamma}$  was changed (stepwise procedure).

Hence, a study of the rheological behavior under steady shear conditions can be confined to the analysis of the shear-dependent properties, defined by the stationary values of the shear stress  $\tau$ .

Flow curves have been obtained over the entire concentration range at 25°C and are reported in Figure 1. For concentrations up to  $C_p = 2.8$ , the limiting zero-shear rate viscosity,  $\eta_0$ , was experimentally attainable, and the shear-dependent behavior of these systems was shear-thinning. For  $C_p > 2.8$ , a change in the slope of the flow curves at low  $\dot{\gamma}$  revealed the appearance of a yield stress,  $\tau_0$ , and the shear-dependent behavior became plastic.

Following the usual procedure for the analysis of the effect of polymer concentration on the rheological properties of polymeric systems, the discussion can be carried out in terms of specific viscosity  $\eta_{sp}$ , defined as:

$$\eta_{sp} = \frac{\eta}{\eta_s} - 1 \quad (4)$$

where  $\eta$  is the steady value of the viscosity of the solution obtained at a given shear rate and  $\eta_s$  is the Newtonian viscosity of the solvent.

Figure 2 shows the dependence of  $\eta_{sp}$  on  $C_p$  in a range of  $\dot{\gamma}$  from 0.9 to 900 s<sup>-1</sup>. As can be seen from Figure 2, lower values of  $\dot{\gamma}$  correspond to a stronger

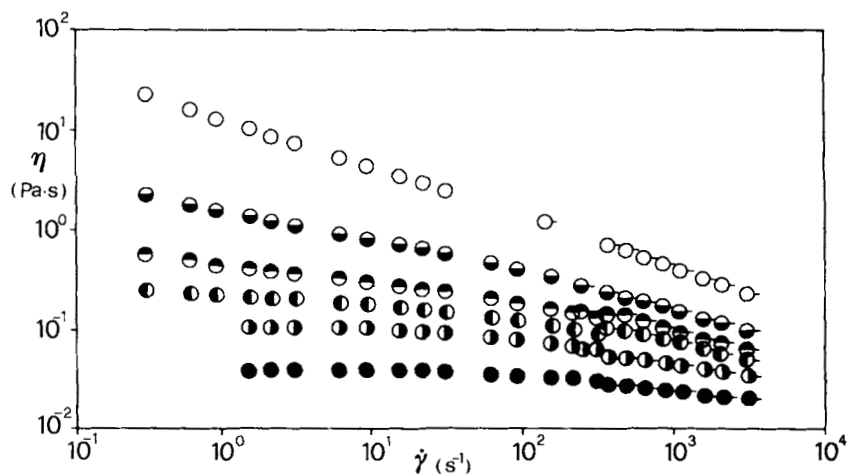


**Figure 1** Flow curves at 25°C and different  $C_p$  values: (●) 2, (○) 2.5, (◐) 2.8, (◑) 3.17, (◒) 4, (○) 6.

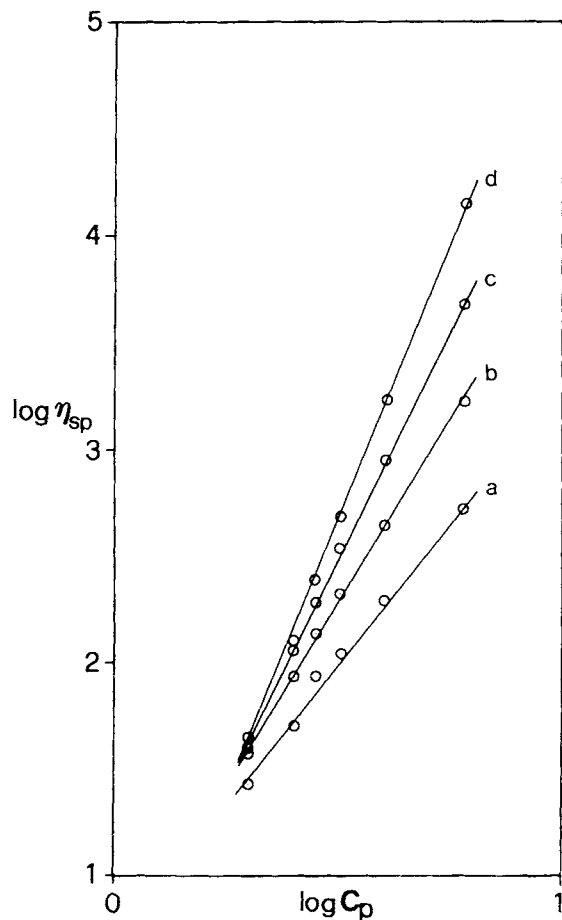


**Figure 2** Specific viscosity vs.  $C_p$  at 25°C and different shear rates: (a) 900 s<sup>-1</sup>, (b) 90 s<sup>-1</sup>, (c) 9 s<sup>-1</sup>, (d) 0.9 s<sup>-1</sup>.

dependence of  $\eta_{sp}$  on  $C_p$ , which can be described by the power-law relation:

$$\eta_{sp} = \alpha C_p^\beta \quad (5)$$

where  $\alpha$  and  $\beta$  are both functions of  $\dot{\gamma}$ .

Figure 3 reports the traces of  $\alpha$  and  $\beta$  as functions of  $\dot{\gamma}$  in the interval of shear rate considered. In this range of  $\dot{\gamma}$ , the exponent  $\beta$ , which accounted for the influence of  $C_p$  on  $\eta$ , regularly increased while decreasing  $\dot{\gamma}$ ; it was not possible to determine an upper limit value for  $\beta$  as  $\dot{\gamma} \rightarrow 0$ . This can be explained considering that, as  $C_p$  increased, the shear-dependent behavior changed in the low shear rate region and the upper limit value of  $\eta$ , the zero-shear-rate viscosity  $\eta_0$ , could not be found for those systems having the higher values of  $C_p$ .

The quantitative analysis of the influence of polymer concentration on the shear-dependent properties of CMS aqueous systems can be easily achieved if carried out on the basis of a limited number of rheological parameters. This implies the definition of a rheological model for the comprehensive description of the shear-dependent behavior of all the systems under investigation.

A constitutive equation, which holds all the required characteristics, can be obtained by adding the plastic term, defined by the yield stress  $\tau_0$ , to the viscous contribution  $\tau_v(\dot{\gamma})$ , expressed by a pseudoplastic model:

$$\tau = \tau_0 + \tau_v(\dot{\gamma}) \quad (6)$$

A suitable pseudoplastic model for the correlation of the experimental data of polymeric solutions is found in the following equation<sup>8</sup>:

$$\tau_v(\dot{\gamma}) = \eta_\infty \dot{\gamma} + \frac{(\eta_0 - \eta_\infty) \dot{\gamma}}{1 + (\lambda \dot{\gamma})^n} \quad (7)$$

which contains four adjustable parameters. If  $n$  assumes a value of  $\frac{2}{3}$  according to Cross,<sup>9</sup> a three-parameter version is obtained, which can be applied successfully to a wide range of pseudoplastic sys-

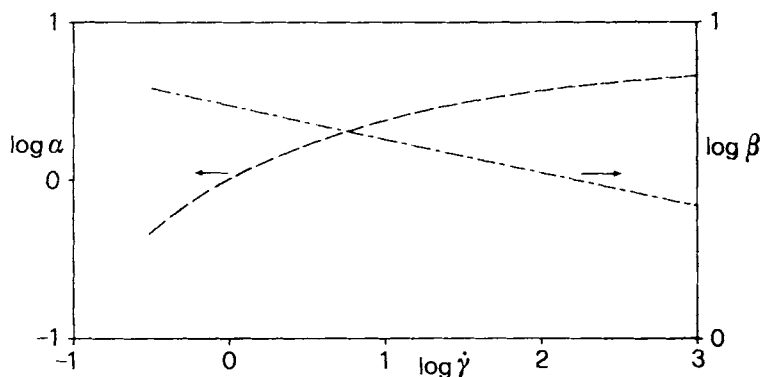


**Figure 3** Shear rate dependence of parameters  $\alpha$  and  $\beta$  [eq. (5)].

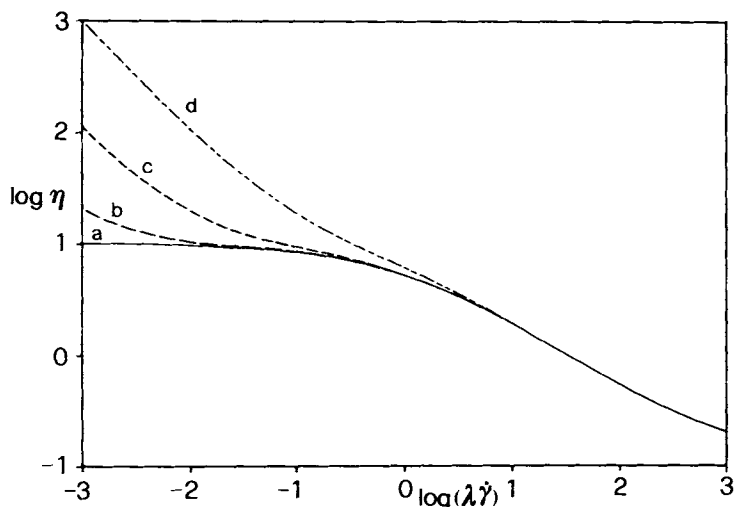


**Figure 4** Flow curves obtained from eq. (8) for different  $\tau_0$  values [ $\eta_0 = 10 \text{ Pa} \times \text{s}$ ;  $\eta_\infty = 0.1 \text{ Pa} \times \text{s}$ ;  $n = \frac{2}{3}$ ; (a)  $\tau_0 = 0 \text{ Pa}$ , (b)  $0.01 \text{ Pa}$ , (c)  $0.1 \text{ Pa}$ , (d)  $1 \text{ Pa}$ ].

tems. Recently, Morris<sup>10</sup> found that the shear-thinning behavior of concentrated solutions of "random coil" polysaccharides can be matched by a two-parameter version of eq. (7) by setting  $n$  to 0.76 and  $\eta_\infty$  to zero.  $\eta_\infty$  is the minimum viscosity that is attained at very high shear rates and cannot be accessed with the conventional rheometers. However, its value can be assumed negligible in comparison with the upper Newtonian viscosity  $\eta_0$ , and, consequently, set to zero or equal to solvent viscosity. The time constant  $\lambda$  is related to shear-thinning onset. Cross<sup>11</sup> suggested identifying  $\lambda$  with a relaxation time, characterizing the viscoelasticity of the system; the inverse of  $\lambda$ ,  $\dot{\gamma}_c = 1/\lambda$ , represents the shear rate at which the viscosity of the system is equal to  $\eta_0/2$ .

Combining the yield stress  $\tau_0$  with the viscous contribution  $\tau_v(\dot{\gamma})$ , expressed by eq. (7), leads to the definition of a model suitable to describe both

shear-dependent behaviors exhibited by the systems examined:

$$\tau = \tau_0 + \eta_\infty \dot{\gamma} + \frac{(\eta_0 - \eta_\infty) \dot{\gamma}}{1 + (\lambda \dot{\gamma})^n} \quad (8)$$

Figure 4 shows how the flow curve calculated from the rheological model gradually changes as a consequence of yield stress variations. Owing to its flexibility, the proposed model can be successfully applied to polymeric systems of different natures and behaviors.<sup>12</sup>

The fitting of the experimental data, obtained at 25°C with eq. (8), gave the results reported in Table I. The  $\eta_\infty$  value was arbitrarily set to 0.001 Pa.s, since for all  $C_p$  there is no evidence for the occurrence of a lower Newtonian plateau in the shear rate range explored.

**Table I** Parameters of Eq. (8), Obtained from Fitting Experimental Data at 25°C

$C_p$ (% w/w)	$\tau_0$ (Pa)	$\eta_0$ (Pa × s)	$\lambda$ (s)	$n$	ARD × 10 <sup>2</sup>
2	0.0065	0.0397	0.00046	0.477	0.58
2.5	0.0124	0.125	0.0030	0.454	0.76
2.8	0.0280	0.240	0.0127	0.379	0.74
3.17	0.0286	0.477	0.0446	0.387	0.69
4	0.234	1.803	0.196	0.446	2.16
6	3.415	17.77	1.168	0.531	1.34

(ARD) fitting average relative deviation.

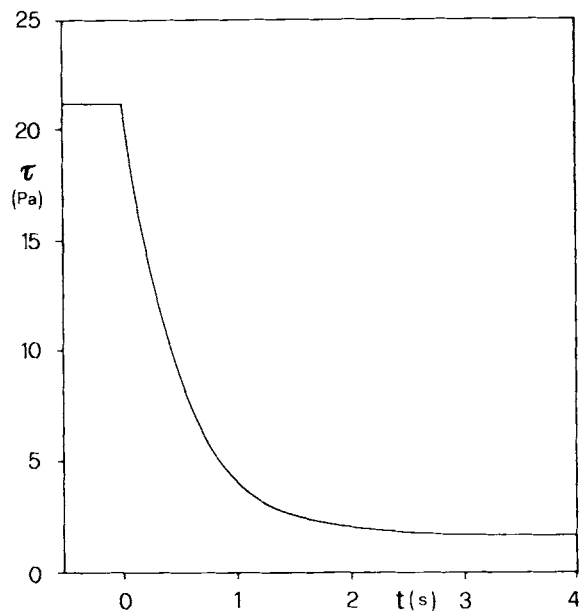


Figure 5 Relaxation test for  $C_p = 6$  (from  $\dot{\gamma} = 3 \text{ s}^{-1}$ ).

For the more concentrated systems, the  $\tau_0$  values derived from data fitting were significantly close to the correspondent residual stresses obtained from relaxation tests. As an example, Figure 5 shows the relaxation curve for the system with  $C_p = 6$ : the residual stress is about 3.5 Pa whereas the calculated  $\tau_0$  is 3.415 Pa.

The parameters  $\tau_0$ ,  $\eta_0$ , and  $\lambda$  increase with increasing  $C_p$ , whereas the exponent  $n$  does not exhibit a monotonic variation. As shown in Figure 6,  $\eta_0(C_p)$  is a continually increasing function of  $C_p$  over the entire concentration range, with a dependence on  $C_p$  of the power-law type:

$$\eta_0 = aC_p^b \quad (9)$$

where  $a = 0.0015$  and  $b = 5.6$ . The concentration dependence of  $\eta_0$ , expressed by eq. (9), is characteristic of polymeric solutions; a value of 3.4 for the exponent  $b$  has been predicted<sup>13,14</sup> and experimentally verified for many concentrated polymeric systems although, for polysaccharides, this value is frequently higher.<sup>15</sup>

For  $\tau_0$  and  $\lambda$ , a transition in the dependence on the polymer concentration can be observed for  $C_p = C_p^* \approx 3.4$  (see Fig. 6). For  $C_p > C_p^*$ , the  $\tau_0$  values are no longer negligible and sensibly increase with  $C_p$ , whereas the characteristic time  $\lambda$  becomes a weaker function of  $C_p$  as the power-law exponent decreases from 10 to 4.4.

The different trends exhibited by  $\tau_0$  and  $\lambda$  for  $C_p > C_p^*$  indicate a change in the physical state of the system, which assumes those characteristics typical of a concentrated disperse system. Hence,  $C_p^*$  represents the threshold concentration value for the pseudoplastic/plastic transition.

The effect of temperature on the shear-dependent behavior of CMS aqueous systems is illustrated in Figure 7, where the flow curves for the system with  $C_p = 2.5$  are reported, as an example, at three different temperatures.

The dependence of  $\eta$  on  $T$  gradually increases with decreasing  $\dot{\gamma}$ , as the curves diverge for  $\dot{\gamma} \rightarrow 0$ . Between 20 and 30°C, a transition from plastic to pseudoplastic behavior can be observed and this results into a  $\tau_0$  reduction to negligible values, as can be seen in Table II.

The same effect of temperature on  $\tau_0$  has been observed for all the systems examined; consequently, a three-dimensional representation of the effect of  $T$  and  $C_p$  on  $\tau_0$ , as shown in Figure 8, can be obtained.

If the change of the rheological behavior is associated with a critical value of  $\tau_0$  it is possible to obtain a curve  $C_p(T)$ , characteristic of the plastic/pseudoplastic transition. The appearance of a yield

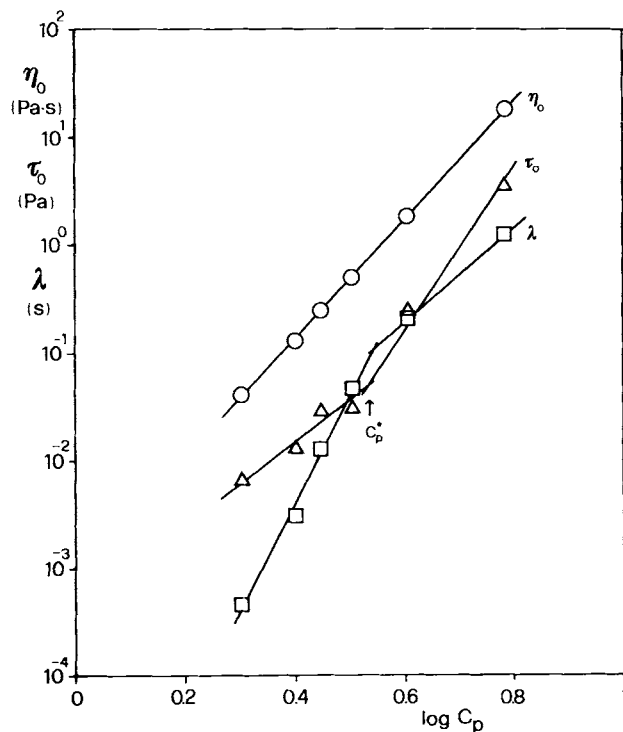
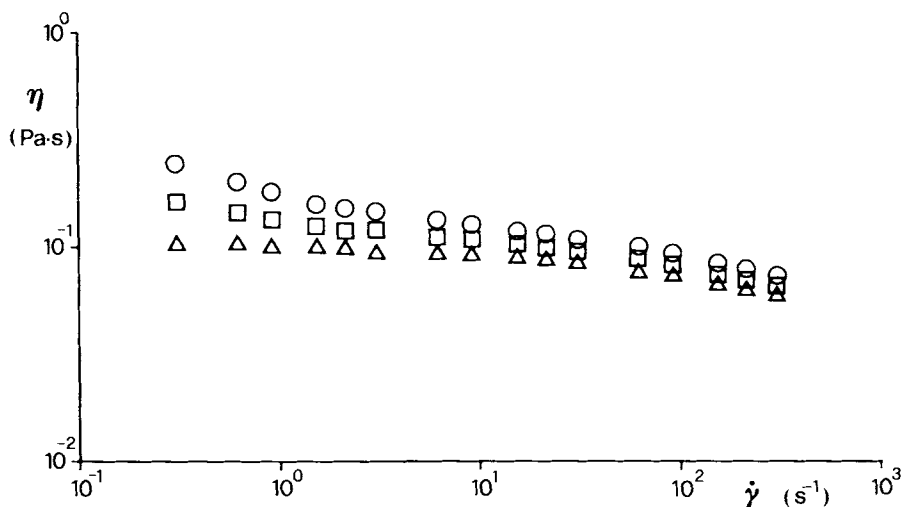


Figure 6 Concentration dependence of parameters  $\eta_0$ ,  $\tau_0$ , and  $\lambda$  at 25°C.



**Figure 7** Effect of temperature on the shear-dependent behavior of the CMS system at  $C_p = 2.5$  [( $\circ$ )  $T = 20^\circ\text{C}$ , ( $\square$ )  $25^\circ\text{C}$ , ( $\triangle$ )  $30^\circ\text{C}$ ].

stress in a disperse system is connected with the formation of a wall-to-wall, three-dimensional network and, consequently, is governed by the numerical density of particles and the aggregation state of the disperse phase. This also explains how polymer concentration and temperature exert their influence on the plastic/pseudoplastic transition.

### Oscillatory Flow Tests

Strain sweeps were performed in order to evaluate the limit of the linear viscoelastic regime, which can be defined by a critical strain value  $\gamma_c^0$ . For  $\gamma^0$  values greater than  $\gamma_c^0$ , a structural breakdown takes place within the material under investigation; hence, measurements at  $\gamma^0 > \gamma_c^0$  can be adopted for an evaluation of structure sensitivity to the imposed strain.

For the CMS system with  $C_p = 2$ , which revealed a typical solution behavior under continuous shear flow conditions, the complex modulus  $G^*$  and the phase shift  $\tau$  are practically independent on the imposed strain  $\gamma^0$ .

By increasing  $C_p$ , the sensitivity to strain increases and reaches a maximum for the most concentrated system ( $C_p = 6$ ).

Figure 9 reports an example of  $G^*$  and  $\delta$  variations with  $\gamma^0$  at two different constant values of  $\omega$ . These traces are typical of structured disperse systems, as they are similar to those exhibited by concentrated suspensions and gels when examined in the same deformation range. Hence, they confirm the peculiarity in the behavior observed for the CMS aqueous systems under continuous shear conditions.

The strong decrease of  $G^*$  with  $\gamma^0$  in the entire range of strain explored seems to indicate that the critical strain of such system is shifted towards very low values of  $\gamma^0$ , sensibly below the lower limit considered. The sensitivity to strain is higher for the elastic component  $G'$  as a result of the variation of  $\delta$  with  $\gamma^0$  (see Fig. 9).

By scanning the imposed frequency of oscillation at constant strain (frequency sweep), the variations of  $G^*$  and  $\delta$  with  $\omega$  can be obtained. In Figure 10, the results obtained from the tests at  $\gamma^0 = 2.4$  are presented as  $\eta^*$  vs.  $\omega$  data: from a comparison of

**Table II** Parameters of Eq. (8), Obtained from Fitting Experimental Data at  $C_p = 2.5$

$T$ ( $^\circ\text{C}$ )	$\tau_0$ (Pa)	$\eta_0$ (Pa $\times$ s)	$\lambda$ (s)	$n$	ARD $\times 10^2$
20	0.0286	0.161	0.0054	0.400	0.63
25	0.0124	0.125	0.0030	0.454	0.76
30	0.0004	0.101	0.0020	0.522	0.45

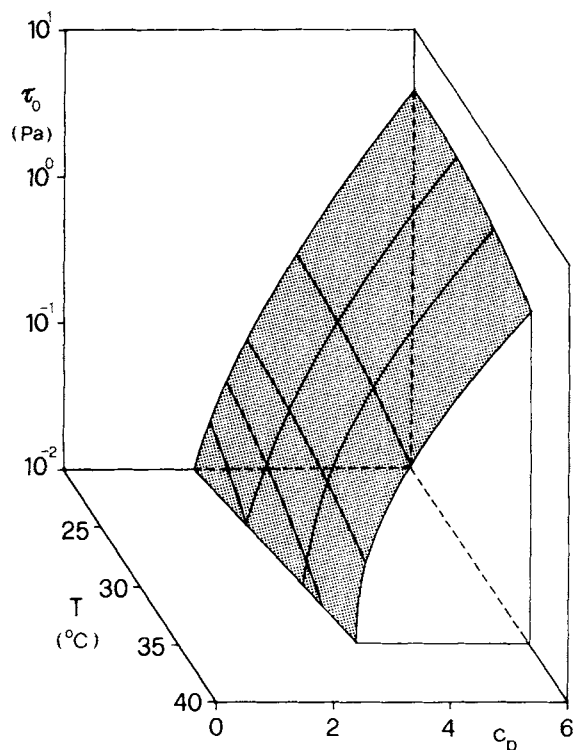


**Figure 8** Dependence of  $\tau_0$  on temperature and polymer concentration.

Figure 10 and Figure 1 it can be observed that the rheological behaviors under oscillatory and continuous shear can be superposed.

This means that, also from the oscillatory flow tests, a progressive modification of the  $\eta^*(\omega)$  curve profiles in the medium-low frequency region emerges with increasing polymer concentration.

For the most concentrated system, the  $\eta^*(\omega)$  curve is similar to that of other systems characterized by long range structures, such as polysaccharide gels, microgels, and aggregated suspensions.

The same conclusions can be drawn from the examination of the mechanical spectra. As can be seen in Figure 11, the frequency dependence of  $G'$  and  $G''$  sensibly modifies in the low frequency region with increasing polymer concentration and, for the most concentrated systems, a low frequency plateau appears, which is typical of structured fluids.

By increasing  $C_p$ , the phase lag  $\delta$  decreases and this concentration dependence of  $\delta$  has been observed for other disperse systems of different natures, such as coal/water slurries.<sup>16</sup> The decrease of  $\delta$  with  $C_p$  becomes larger for lower strain values; for example, at  $\omega = 1.9$  rad/s and  $\gamma^0 = 0.24$ ,  $\delta$  changes from 1.19 to 0.92 rad, whereas, at  $\gamma^0 = 1.4$ ,  $\delta$  decreases from 1.43 to 1.32 rad.

The variations of the storage and loss moduli,  $G'$  and  $G''$ , with  $\omega$  can be correlated with the relaxation spectra  $H(\lambda)$  through the following relationships:

$$G'(\omega) = \int_{-\infty}^{+\infty} H(\lambda) \frac{\omega^2 \lambda^2}{1 + \omega^2 \lambda^2} d \ln \lambda \quad (10)$$

$$G''(\omega) = \int_{-\infty}^{+\infty} H(\lambda) \frac{\omega \lambda}{1 + \omega^2 \lambda^2} d \ln \lambda \quad (11)$$

It follows that the concentration and temperature effects on the viscoelastic properties of the CMS systems considered can be interpreted as modifications in the corresponding relaxation spectra.

Several methods<sup>17</sup> can be applied for the calculation of  $H(\lambda)$  from  $G'(\omega)$  and  $G''(\omega)$  experimental data. In the present article, the procedure suggested by Ninomiya and Ferry<sup>18</sup> was selected for its simplicity, since no derivative calculation is required but only values of  $G'$  or  $G''$  spaced at equal intervals on a logarithmic frequency scale.

Under the experimental conditions employed,  $G''(\omega)$  represents the major component of the complex modulus  $G^*(\omega)$ ; consequently, the relaxation spectra have been calculated from the following equation:

$$H(\lambda) = \frac{2}{\pi} \left[ G''(\omega) - \frac{c}{(c-1)^2} [G''(c\omega) + G''(\omega/c) - 2G''(\omega)] \right]_{1/\omega=\lambda} \quad (12)$$

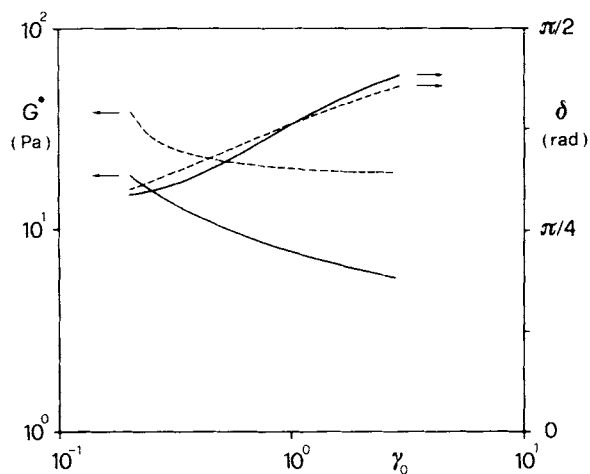


**Figure 9** Strain dependence of the complex modulus  $G^*$  and the phase shift  $\delta$  for  $C_p = 6$  at  $25^\circ\text{C}$  and two different frequencies [(-----) 0.628 rad/s, (—) 6.28 rad/s].



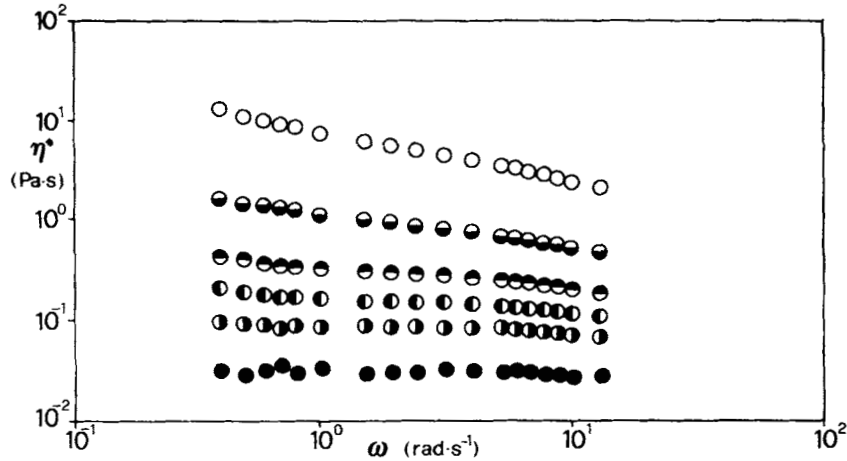


**Figure 10** Frequency dependence of the complex viscosity  $\eta^*$  at 25°C,  $\gamma^0 = 2.4$  and different  $C_p$  values: (●) 2, (○) 2.5, (●) 2.8, (○) 3.17, (○) 4, (○) 6.

where the scaling factor  $c$  was set equal to  $10^{0.2}$ .<sup>18</sup> Figure 12 reports the relaxation spectra obtained for four selected  $C_p$  values, at 25°C. As  $C_p$  increases, the profile of  $H(\lambda)$  becomes asymptotic at high  $\lambda$  values and can be described by

$$H(\lambda) = A + B\lambda^{-m} \quad (13)$$

$H(\lambda)$  reduces to a box-type distribution for high relaxation times as a consequence of the low frequency plateau observed for  $G''$ , which, in turn, is

connected with the aggregation of the disperse phase, typical of high  $C_p$  values. The degree of aggregation is strongly dependent upon the deformation conditions imposed to the system. Figure 13 shows the  $H(\lambda)$  modifications induced by an increase of  $\gamma^0$  in the high relaxation time interval. Higher  $\gamma^0$  values produce a partial breakdown of the structural network, which results in a reduction of the box-type contribution given by the parameter  $A$  in eq. (13).

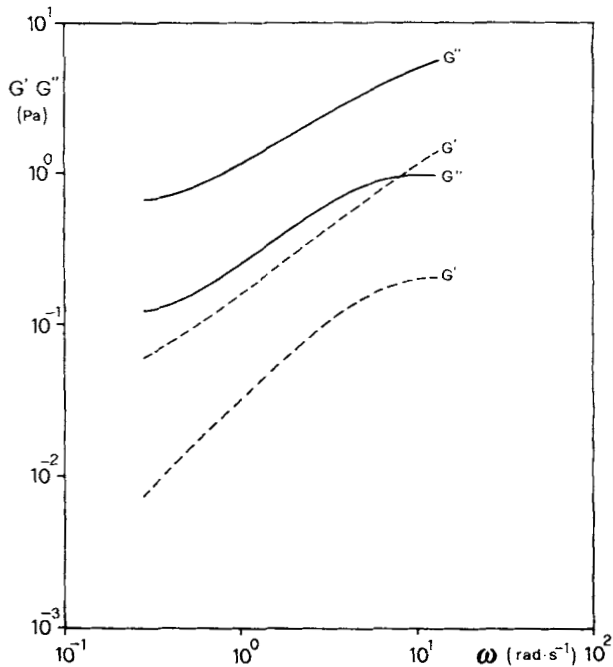


**Figure 11** Mechanical spectra for  $C_p = 2.8$  (-----) and 4 (—).

### CONCLUSIONS

The rheological behavior of the CMS aqueous systems examined is typical of disperse systems having a weak degree of particle aggregation, as can be ar-

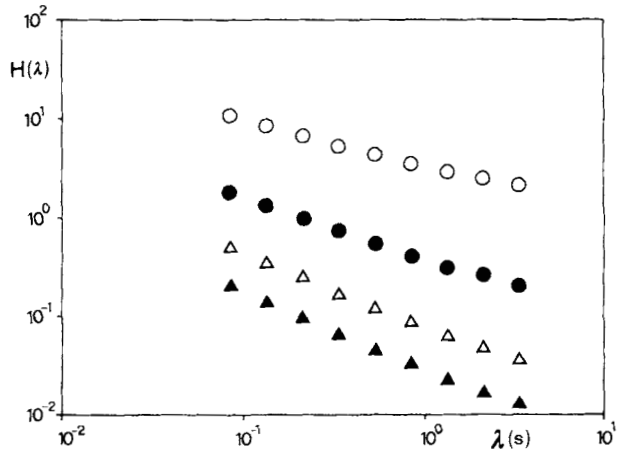


**Figure 12** Relaxation spectra derived from  $G''(\omega)$  data at  $\gamma^0 = 2.4$  and 25°C, for four different  $C_p$  values: (▲) 2.8, (△) 3.17, (●) 4, (○) 6.

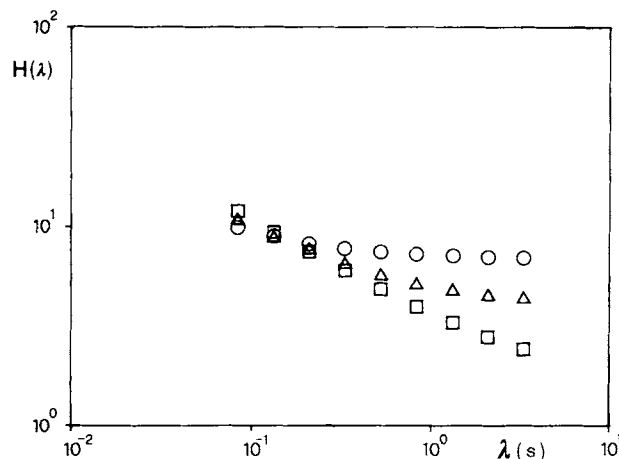


**Figure 13** Relaxation spectra for  $C_p = 6$ , at  $20^\circ\text{C}$  and three different  $\gamma^0$  [( $\circ$ ) 0.24, ( $\triangle$ ) 0.48, ( $\square$ ) 2.4].

gued from both the continuous and oscillatory flow tests.

The degree of aggregation of the disperse phase is essentially governed by numerical particle density and particle interactions. Consequently, polymer concentration and temperature exert a strong influence on the properties of CMS systems and, eventually, give rise to a transition in the rheological behavior under continuous and oscillatory flow conditions.

Above a critical polymer concentration, whose value depends on temperature, the formation of a three-dimensional continuous network in the disperse phase occurs in rest conditions, as can be deduced from the appearance of a yield stress in continuous flow curves and a finite plateau in the low frequency region of mechanical spectra.

A rheological model is proposed for the correlation of continuous shear data, which enables the evaluation of the yield stress  $\tau_0$  and, hence, the definition of the concentration and temperature conditions for the pseudoplastic/plastic transition.

The moderate degree of connectivity of the three-dimensional network, even at the highest concentration and lowest temperature considered, is confirmed by the relatively low  $\tau_0$  values, if compared

with those of other structured systems, and by the high strain sensitivity of the viscoelastic quantities. The strain effects, as well as the strong influence of polymer concentration and temperature, can be clearly illustrated through the modifications of the relaxation spectra, calculated from  $G''(\omega)$  data, in the high relaxation time interval.

## REFERENCES

1. A comprehensive bibliography on polysaccharides is reported in: (a) *The Polysaccharides*, G. O. Aspinall, Ed., Academic, New York, 1983, and (b) M. Yalpani, *Polysaccharides: Syntheses, Modifications and Structure/Property Relations*, Elsevier, Amsterdam, 1988.
2. S. Ring and G. Stainsby, *Progress in Food and Nutrition Science*, **6**, 323 (1982).
3. J. H. Chowdhury, *Biochem. Z.*, **148**, 76 (1924).
4. W. F. Filbert, U.S. Patent 2,599,620 (August 31, 1950).
5. H. S. Roberts, in *Starch: Chemistry and Technology*, Vol. II, R. L. Whistler and E. F. Paschall, Eds., Academic, New York, 1967, pp. 316-343.
6. F. Wolf and G. Bahmann, East Germany Patent 103,646 (May 4, 1974).
7. N. W. Taylor, *J. Appl. Polym. Sci.*, **24**, 2031 (1979).
8. M. M. Cross, *J. Colloid Sci.*, **20**, 417 (1965).
9. M. M. Cross, *J. Appl. Polym. Sci.*, **13**, 675 (1969).
10. E. R. Morris, *Carbohydr. Polym.*, **13**, 85 (1990).
11. M. M. Cross, *Rheol. Acta*, **18**, 609 (1979).
12. R. Lapasin, S. Pricl, and P. Esposito, in *Rheology of Food, Pharmaceutical and Biological Materials with General Rheology*, R. E. Carter, Ed., Elsevier Applied Science, London, New York, 1990, pp. 122-132.
13. W. W. Graessley, *Adv. Polym. Sci.*, **16**, 1 (1974).
14. P. G. de Gennes, *Nature (London)*, **282**, 367 (1979).
15. G. Robinson, S. B. Ross-Murphy, and E. R. Morris, *Carbohydr. Res.*, **107**, 17 (1982).
16. R. Lapasin and S. Pricl, *Can. J. Chem. Eng.*, **70**, 20 (1992).
17. J. D. Ferry, *Viscoelastic Properties of Polymers*, Wiley, New York, London, 1980.
18. K. Ninomiya and J. D. Ferry, *J. Colloid Sci.*, **14**, 36 (1959).

Accepted February 4, 1991